# FISEVIER

#### Contents lists available at ScienceDirect

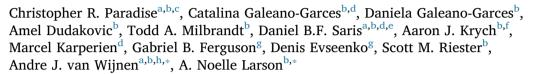
### Gene

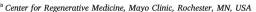
journal homepage: www.elsevier.com/locate/gene



#### Research paper

# Molecular characterization of physis tissue by RNA sequencing<sup>★</sup>





<sup>&</sup>lt;sup>b</sup> Department of Orthopedic Surgery, Mayo Clinic, Rochester, MN, USA

#### ARTICLEINFO

#### Keywords: Physis Growth plate RNA sequencing Bone Cartilage

#### ABSTRACT

The physis is a well-established and anatomically distinct cartilaginous structure that is crucial for normal longbone development and growth. Abnormalities in physis function are linked to growth plate disorders and other pediatric musculoskeletal diseases. Understanding the molecular pathways operative in the physis may permit development of regenerative therapies to complement surgically-based procedures that are the current standard of care for growth plate disorders. Here, we performed next generation RNA sequencing on mRNA isolated from human physis and other skeletal tissues (e.g., articular cartilage and bone; n=7 for each tissue).

We observed statistically significant enrichment of gene sets in the physis when compared to the other musculoskeletal tissues. Further analysis of these upregulated genes identified physis-specific networks of extracellular matrix proteins including collagens (COL2A1, COL6A1, COL9A1, COL14A1, COL16A1) and matrilins (MATN1, MATN2, MATN3), and signaling proteins in the WNT pathway (WNT10B, FZD1, FZD10, DKK2) or the FGF pathway (FGF10, FGFR4). Our results provide further insight into the gene expression networks that contribute to the physis' unique structural composition and regulatory signaling networks. Physis-specific expression profiles may guide ongoing initiatives in tissue engineering and cell-based therapies for treatment of growth plate disorders and growth modulation therapies. Furthermore, our findings provide new leads for therapeutic drug discovery that would permit future intervention through pharmacological rather than surgical strategies.

#### 1. Introduction

Leg length discrepancy and angular limb deformities are common pediatric disorders that result in pain, limp and potential lifelong disability. To treat growth plate or physeal disorders, children frequently require complex surgical reconstructions to alleviate symptoms and restore functional capacity. Current treatments include manipulation of the growth plate by surgically tethering or ablating the physis, resection of damaged portions of the growth plate to restore growth, and limb lengthening procedures using distraction osteogenesis (Sanders et al.

Abbreviations: NCATS, National Center for Advancing Translational Sciences; NIH, National Institutes of Health; COL2A1, collagen Type II alpha 1 chain; COL6A1, collagen type VI alpha 1 chain; COL9A2, collagen type IX alpha 2 chain; COL9A3, collagen type IX alpha 3 chain; COL11A2, collagen type XI alpha 1 chain; COL16A1, collagen type XI alpha 1 chain; COL16A1, collagen type XI alpha 1 chain; MATN1, Matrilin 1; MATN2, Matrilin 2; MATN3, Matrilin 3; WNT10B, Wnt Family Member 10B; FZD1, frizzled class receptor 1; FZD2, frizzled class receptor 2; FZD10, frizzled class receptor 10; DKK1, Dickkopf WNT signaling pathway inhibitor 2; FGF, fibroblast growth factor; FGF10, fibroblast growth factor 18; FGFR4, fibroblast growth factor receptor 4; RT-qPCR, real-time quantitative polymerase chain reaction; RNA-seq, mRNA sequencing; IRB, institutional review board; SRA, Sequence Read Archive; RIN, RNA Integrity Number; RPKM, reads per kilobasepair per million mapped reads; IHC, immunohistochemistry; BSA, bovine serum albumin; DAB, 3,3′-diaminobenzidine; PCA, principal component analysis; GO, gene ontology; EDS, Ehlers-Danlos Syndrome; ANOVA, analysis of variance; HBB, hemoglobin β



<sup>&</sup>lt;sup>c</sup> Mayo Clinic Graduate School of Biomedical Sciences, Mayo Clinic, Rochester, MN, USA

<sup>&</sup>lt;sup>d</sup> Department of Developmental BioEngineering, University of Twente, Enschede, Netherlands

e Department of Orthopaedics, University Medical Center Utrecht, Utrecht University, Utrecht, Netherlands

f Department of Sports Medicine, Mayo Clinic, Rochester, MN, USA

<sup>&</sup>lt;sup>8</sup> Department of Orthopaedic Surgery, University of Southern California (USC), Los Angeles, CA, USA

h Department of Biochemistry and Molecular Biology, Mayo Clinic, Rochester, MN, USA

Institution where reported work was done: Mayo Clinic, Rochester, MN, USA.

<sup>\*</sup> Corresponding authors at: Mayo Clinic, 200 First Street SW, Rochester, MN 55905, USA.

E-mail addresses: vanWijnen.Andre@mayo.edu (A.J. van Wijnen), Larson.Noelle@mayo.edu (A. Noelle Larson).

C.R. Paradise et al. Gene 668 (2018) 87-96

2007; Stevens 2007; Black et al. 2015; Clark et al. 2015). Although deformities can be corrected using these techniques, they are not always effective and are associated with significant complications such as infection, nerve injury, fracture, and morbidity (Hantes et al. 2001; Launay et al. 2013). Novel strategies such as administration of local pharmacologic agents aimed at selectively enhancing or inhibiting the growth plate function have the potential to improve the clinical outcomes over current treatments by avoiding the pain and morbidity associated with complex surgical reconstructions.

The physis is a unique cartilaginous structure that is responsible for the longitudinal growth of long bones via the process of endochondral ossification (Kronenberg 2003). As a transition zone between resting chondrocytes and newly calcified bone matrix, the physis is comprised of several distinct layers (Marino 2011). Briefly, the reserve or germinal zone contains chondrocyte progenitor cells and resting chondrocytes. This zone is adjacent to the zone of proliferation where chondrocytes multiply and form the classic columnar arrangement before entering the zone of hypertrophy. At this stage, chondrocytes increase in size and reach a terminally differentiated state culminating in cell apoptosis. Osteoblasts fill this void and begin to calcify the extracellular matrix to form the zone of ossification. Longitudinal growth of long bones is mediated by the proliferation of resting chondrocytes and their subsequent hypertrophy (Andrade et al. 2010; Lui et al. 2010). This transition is associated with an increase in extracellular matrix production controlled by a complex regulatory network (Myllyharju 2014). Thus, the growth plate serves as a dynamic transitional tissue between resting chondrocytes and newly formed cortical bone.

Better understanding of the gene expression profile and signaling patterns within the physis may elucidate novel regulatory pathways involved in physis maturation and long-bone development. Insight gained from such an analysis can be leveraged for tissue engineering strategies and/or identification of drug targets for therapeutics aimed to modulate growth plate function. Previous studies from our group and others have demonstrated the utility of mRNA analysis (i.e. RT-qPCR and/or RNA-sequencing) as a means to identify key regulatory gene networks within specific musculoskeletal tissue types or disease states (Lewallen et al. 2016; Lin et al. 2016; Galeano-Garces et al. 2017; Riester et al. 2017). Thus, we sought to identify differentially expressed mRNA transcripts in the physis compared to other musculoskeletal tissues. We provide a detailed comparative analysis of RNA sequencing data derived from physis tissue compared to bone, articular cartilage, and muscle. Further analysis of these differentially expressed genes reveals structural components and signaling pathways distinct to the physis.

#### 2. Methods

#### 2.1. RNA extraction from tissues

Tissue specimens were collected from patients undergoing tissue removal as part of planned surgical procedures (Supplemental Table 1). Each sample was obtained from a different patient with the exception of one matched cartilage and bone sample and another matched pair of physis samples as indicated in the supplementary table. The specimens used in this investigation were collected under institutional review board (IRB) approved protocols (IRB# 13-005403 and 13-005619). Written informed consent was obtained for all biospecimens that were collected. Expression data for two of the samples included in the muscle group were obtained from the Sequence Read Archive (SRA) database (accession numbers SRR1424734 and SRR1424735) (Lindholm et al. 2014).

At the time of surgical harvest, tissues were snap frozen in liquid nitrogen and stored at  $-80\,^{\circ}\text{C}$ . For bone, articular cartilage, and muscle, frozen tissue biopsies were ground into a powder using a mortar and pestle and homogenized in Qiazol reagent (Qiagen, Hilden, Germany). Total RNA was extracted from research biopsies using the

RNeasy minikit (Qiagen, Hilden, Germany) and quantified using the NanoDrop 2000 spectrophotometer (Thermo Fischer Scientific, Wilmington, Delaware). For growth plate specimens, RNA was isolated from the frozen biopsies using AnaPrep Total RNA Extraction Kit (Biochain, Newark, CA) and quantified using the NanoDrop 2000 spectrophotometer (Thermo Fischer Scientific, Wilmington, Delaware). For samples selected for next generation sequencing, RNA integrity was assessed using the Agilent Bioanalyzer DNA 1000 chip (Invitrogen, Carlsbad, CA). Only samples with an RNA Integrity Number (RIN) and DV<sub>200</sub> score greater than our Sequencing Core's minimum cutoff (RIN > 6 and DV<sub>200</sub> > 50%) were used for sequencing.

#### 2.2. Next generation mRNA sequencing

RNA sequencing and subsequent bioinformatic analysis were performed in collaboration with the Mayo Clinic RNA sequencing and bioinformatics cores as previously described (Dudakovic et al. 2014; Kalari et al. 2014). In brief, library preparation was performed using the TruSeq RNA library preparation kit (Illumina, San Diego, CA). Polyadenylated mRNAs were selected using oligo dT magnetic beads. TruSeq Kits were used for indexing to permit multiplex sample loading on the flow cells. Paired-end sequencing reads were generated on the Illumina HiSeq 2000 sequencer. Quality control for concentration and library size distribution was performed using an Agilent Bioanalyzer DNA 1000 chip and Qubit fluorometry (Invitrogen, Carlsbad, CA). Sequence alignment of reads and determination of normalized gene counts were performed using the MAP-RSeq (v.1.2.1) workflow, utilizing TopHat 2.0.6 (Kim et al. 2013), and HTSeq (Anders et al. 2015). Normalized read counts were expressed as reads per kilobasepair per million mapped reads (RPKM). For muscle samples, raw read counts were obtained from the GEO database (accession#: GSE60591) and these counts were subjected to the same bioinformatic process as the samples obtained in this study.

#### 2.3. Computational analysis and statistics

Normalized read counts generated from the RNA sequencing data were analyzed to assess differential gene expression between growth plate, articular cartilage, bone, and muscle specimens. Genes with an RPKM value > 0.3 in at least one tissue type were included in subsequent computational analyses. Discovery of differentially expressed genes (Physis vs. Bone/Cartilage/Muscle) was determined using the Two-stage linear step-up procedure of Benjamini, Krieger and Yekutieli with Q = 5% in GraphPad Prism version 7.03 for Windows. A volcano plot was generated using R Version 3.4.0 (Team 2017). Venn Diagrams were generated using InteractiVenn online tool (Heberle et al. 2015). Functional annotation clustering of differentially expressed genes was performed using DAVID Bioinformatics Resources 6.8 database (DAVID 6.8) (Shannon et al. 2003, da Huang et al., 2009). GO Term networks were created using the ClueGO plug-in within the Cytoscape software environment (Shannon et al., 2003, Bindea et al. 2009). Hierarchical clustering was performed using Morpheus matrix visualization and analysis software after a Log2 adjustment was made for each gene row (Broad Institute). Protein-protein interaction networks were generated using STRING Database version 10.5 (Szklarczyk et al. 2015; Szklarczyk et al. 2017).

#### 2.4. Histological analysis

All tissues were fixed overnight in 10% neutral buffered formalin. Then, samples were washed and dehydrated in graded series of ethanol (70% to 100%) and processed with xylene (50% to 100%) prior to paraffin embedding. Paraffin blocks were cut into consecutive sections of  $5\,\mu m$  thickness using a microtome and placed onto charged microscope glass slides for histological staining. Following deparaffinization, sections were stained for proteoglycan content using 0.125% safranin-O

## Download English Version:

# https://daneshyari.com/en/article/8644783

Download Persian Version:

https://daneshyari.com/article/8644783

<u>Daneshyari.com</u>